Sensors and Actuators B 203 (2014) 612–620

Contents lists available at ScienceDirect

Sensors and Actuators B: Chemical

journal homepage: www.elsevier.com/locate/snb

Diphenylanthrylene and diphenylfluorene-based segmented conjugated polymer films as fluorescent chemosensors for nitroaromatics in aqueous solution

Pablo G. Del Rosso[a], Maria J. Romagnoli[a], Marcela F. Almassio[a], Cesar A. Barbero[b], Raúl O. Garay[a,*]

[a] INQUISUR, Departamento de Química, Universidad Nacional del Sur, Alem 1253, CP 8000 Bahía Blanca, Argentina
[b] Departamento de Química, Facultad de Ciencias Exactas, Fisicoquímicas y Naturales, Universidad Nacional de Río Cuarto, Agencia Postal No 3, CP5800 Río Cuarto, Argentina

ARTICLE INFO

Article history:
Received 23 May 2014
Accepted 9 July 2014
Available online 17 July 2014

Keywords:
Fluorescence quenching
Segmented conjugated polymer
Nitroaromatics
Film sensor
Aqueous phase

ABSTRACT

A new regularly segmented conjugated polymer with diphenylanthryl chromophores bearing oxyethylene side chains was synthesized. The amorphous polymer was solution-processable. The formation of aggregated species in solid phase was hindered by the bent microstructure while fluorescence depolarization measurements showed high exciton mobilities among the short chromophores. The fluorescence quenching of films of **PA** toward nitroaromatics in aqueous solution was evaluated and compared with the behavior of **PF**; a diphenylfluorenylene-based segmented CP bearing non-polar aliphatic side chains. Films of both polymers exhibit remarkable sensing abilities in the micromolar range thus showing that hydrated films have porosity at the molecular level. The fluorene-based **PF** had higher overall quenching responses to NACs than the anthryl-based **PA** while nitrophenols were more effective than nitrotoluenes in quenching the fluorescence of both **PA** and **PF**. Such differences are rationalized in terms of polymer–analyte interactions. The binding strengths between analytes and sensing materials were evaluated by their Hansen solubility parameters. We concluded that strong analyte cohesive interactions with the polymer could drag analyte diffusion and impair polymer sensing ability and should be avoided in the design of responsive polymers to be used in the present sensing configuration.

1. Introduction

Nitro aromatic compound (NAC) sensing is necessary for environmental pollution control, security matters and industrial applications [1–3]. For instance, phytotoxic nitrophenols are primary and secondary pollutants found in air, dew and rain in city downtown and industrial areas [4]. In addition, the characterization of soil and groundwater at munitions production, distribution and storage facilities usually reveals contamination with toxic nitrotoluene derivatives. Chemosensing methods based in responsive polymers have raised interest because of high sensitivity, stability, reproducibility, affordability and feasibility for miniaturization [5,6]. Thus, fluorescent quenching of conjugated macromolecular films is a promising approach for detection of NACs because they display sensory signal amplification by energy migration along the conjugated polymer (CP) chain. The best sensory responses in solid state have been observed when bulky groups attached to the CP main chain bring porosity to the films that foster analyte diffusion into the sensing layer [7,8]. However, luminescent molecular structures such as dendrimers [9,10] or hyperbranched polymers [11] or monolayers [12,13] that also facilitate fluorophore–quencher interactions have proven to be very sensitive toward nitroaromatics.

Our approach to generating film porosity involves the use of CPs with broken conjugation whose microstructure consists of conjugated aromatic segments tethered along the main chain by saturated 2,2-isopropylene spacers; the latter structural motif induced twisted arrangements of the attached geminal fluorophores [14]. The contorted conformations adopted by the regularly segmented CP main chain produce amorphous morphologies, introduce porosity of molecular dimensions and reduce any potential π-stacking that usually leads to polymer self-quenching. Thus, previous reports from our group detailed the high quenching sensitivity of these new segmented CPs toward methanolic solutions of NACs thus demonstrating the amplified quenching effect

* Corresponding author. Tel.: +54 291 4595101; fax: +54 291 4595187.
E-mail address: rgaray@criba.edu.ar (R.O. Garay).

http://dx.doi.org/10.1016/j.snb.2014.07.032
0925-4005/

that an array of structurally well-defined chromophoric units can display in solid state [15,16]. We also encountered in these studies the difficulties already mentioned by other authors [13,17] in establishing trends for quenching responses of NACs in condensed phase, e.g, films of a quaterphenylene-based segmented CP were very sensitive toward picric acid but showed no response to trinitrotoluene [16]. Although these empirical types of findings could be of interest for the design of selective sensors, their serendipity makes them less valuable in building a rationale for polymer tailoring.

In this paper we selected two sets of NACs with increasing molecular volume and decreasing reduction potential for our experiments in order to implement a more systematic approach to studying the quenching efficiency of phytotoxic nitrophenols and nitrotoluene derivatives. The first set was composed of nitrophenol (NP), dinitrophenol (DNP) and trinitrophenol (TNP) while the second one was constituted by nitrotoluene (NT), dinitrotoluene (DNT) and trinitrotoluene (TNT). We also report herein the synthesis and electro-optical characterization of a new amorphous diphenylanthrylene-based segmented CP bearing polar oxyethylene side chains, **PA**, see Scheme 1. Its electrochemical and photophysical properties were investigated using cyclic voltammetry (CV) and both UV–visible absorption and steady state photoluminescence emission (PL) spectroscopies. Then, the fluorescence quenching response of hydrated films of **PA** to the two series of NACs in aqueous solution was evaluated and the results were compared with those obtained in similar quenching experiments with a diphenylfluorenylene-based segmented CP bearing non-polar aliphatic side chains, **PF**, in order to observe whether either the polymer bearing polar side chains or the one with the non polar chains show selectivity to either one of the two NAC sets.

2. Experimental

2.1. General methods and instrumentation

Melting points reported are not corrected. ^{1}H NMR and ^{13}C NMR spectra were recorded on a Bruker ARX300 spectrometer on samples dissolved in $CDCl_3$. Mass spectra were measured with Varian MAT CH-7A instrument. Gel permeation chromatography analyses were carried out on THF solutions at room temperature using a Waters model 600 furnished with a Waters 2487 UV detector set at 254 nm. Calibration of the instrument was done using polystyrene standards. Thermal analysis was carried out on a TA Q20 instrument under nitrogen flow at a scan rate of 10 °C/min. The thermal behavior was observed on an optical polarizing microscope (Leitz, Model Ortolux) equipped with a hot stage (Mettler).

UV/vis spectra were obtained from a UV–visible GBC Cindra 20 spectrometer. The absorption measurements were done either on dilute samples (less than 0.01 g/ml) or on thin films cast on quartz plates, which were placed at a 30° angle with respect to the incident beam. The molar extinction coefficients (e) were obtained from the slope of the plot of the absorption with six solutions of different concentrations vs. the concentration (correlation values ^{3}0.99). Steady-state fluorescence studies were conducted using an SML AMINCO 4800 spectrofluorimeter at 25 °C. The emission measurements were carried out on dilute samples (less than 0.02 mg/ml) using a quartz cuvette with a path length of 1 cm and keeping the optical densities below 0.1 to minimize aggregation and reduce artifacts introduced by self-absorption in fluorescence. Thin film spectra were recorded by front-face (30°) detection. Film specimens were drop-cast from a $CHCl_3$ solution on quartz substrates and dried at room temperature. Fluorescence anisotropy was measured using a couple of film polarizers on the excitation and emission beams in the spectrofluorimeter operating in an L-format. The fluorescence anisotropy is calculated according to $<r> = I_{vv} - GI_{vh}/(I_{vv} + G2I_{vh})$ where $I_{exc,em}$ is the intensity of the emission, v and h are the vertical or horizontal alignment of the excitation and emission polarizers, and $G = I_{hv}/I_{hh}$ is the instrumental correction factor which accounts for the difference in sensitivities for the detection and emission in the perpendicular and parallel polarized configurations [27].

Electrochemistry experiments were performed in a Bas Epsilon instrument with a three-electrode setup using platinum wire as working electrode, a Pt wire as counter electrode and Ag wire on which AgCl had been deposited electrolytically as the reference electrode. Cyclic voltammograms were recorded potentiostatically in CH_2Cl_2 with 0.1 M tetraethylammonium perchlorate as supporting electrolyte at a scan rate of 100 mV/s.

2.2. Materials and synthesis

Melting points reported are not corrected. 2,6-Dihydroxy-9,10-anthraquinone, bisphenol A, 1,4,7-trioxanonanol and other reagents were purchased from Aldrich and used without further purification unless otherwise specified. THF was purified by distillation from Na/benzophenone. Tetrakis(triphenylphosphine)palladium(0) was prepared from literature [18,19]. 2,4,6-Trinitrotoluene was prepared as reported elsewhere [20] and recrystallized three times from ethanol.

2.2.1. Monomer synthesis

The synthesis of the monomer 2,2-bis[3-(1,3,2-dioxaborinan-2-yl)-4-methoxyphenyl] propane has been already reported [15]. 1,4,7-Trioxanonyl-*p*-toluenesulfonate was prepared according to a reported procedure [21].

*2.2.1.1. 2,6-Dihydroxyanthracene (**1**).* A suspension of 2,6-dihydroxy-9,10-anthraquinone (20 g; 83 mmol) in 25% aqueous solution of ammonia (190 ml) was treated with Al(Hg) (6.0 g) and heated under reflux for 5 h. After cooling at r.t., 35% HCl (200 ml) was added and the precipitate was collected by filtration. The product was extracted in a sohxlet with 2-butanone and then the solvent was evaporated. The product (11.5; 65%) was used as such in the next step. M.p. 287 °C (decomp.). ^{1}H NMR (acetone-d_6) d 8.51 (s, 1H), 8.17 (s, 1H), 7.88 (d, 1H, J = 9.0 Hz), 7.26 (d, 1H, J = 2.5 Hz), 7.19 (dd, 1H, J = 9.0 Hz and 2.5 Hz); ^{13}C NMR (acetone-d_6) d 154.8, 132.5, 130.2, 129.6, 124.4, 121.1, 108.1.

*2.2.1.2. 2,6-Bis(1,4,7-trioxanonyl)anthracene (**2**).* A mixture of **1** (7.37 g; 35 mmol) and sodium hydride (2.11 g) was dissolved with DMF (50 ml) and after the hydrogen evolution totally receded, ca. 15 min, a solution of 1,4,7-trioxanonyl-*p*-toluenesulfonate (7.3 g; 25.3 mmol) in DMF (50 ml) was added at r.t. The green mixture was heated under reflux for 3 h. After standing overnight at r.t. the product was collected by filtration, washed with benzene (3× 30 ml) and dissolved in $CHCl_3$ (750 ml). The solution was washed with 10% NaOH (40 ml), 5% $NaHCO_3$ (50 ml), brine (50 ml), dried with Na_2SO_4, and evaporated. Crystallization at 4 °C of the residue from acetone (150 ml) afforded **5** (10.78 g, 69%). M.p. 131–132 °C. ^{1}H NMR ($CDCl_3$) d 8.15 (s, 1H), 7.81 (d, 1H, J = 10.1), 7.16 (m, 2H), 4.27 (t, 2H, J = 4.9 Hz), 3.93 (t, 2H, J = 4.9 Hz), 3.75 (m, 2H), 3.62 (m, 2H), 3.52 (q, 2H, J = 7.0 Hz), 1.21 (t, 3H, J = 7.0 Hz); ^{13}C NMR ($CDCl_3$) d 155.9, 131.4, 129.4, 129, 124.5, 120.9, 105.1, 71.2, 70.1, 70.0, 67.6, 66.9, 15.3; MS (70 eV), m/z (%), 443 (M^++1, 26), 442 (M^+, 100), 441 (24), 210 (96), 181 (27), 117 (58), 89 (20), 73 (79). Anal. Calcd. for $C_{26}H_{34}O_6$ C, 70.56; H, 7.74. Found C, 70.45; H, 7.64.

*2.2.1.3. 9,10-Dibromo-2,6-bis(1,4,7-trioxanonyl)anthracene (**3**).* A solution of Br_2 (7,2 g; 45 mmol) in CH_2Cl_2 (65 ml) was added drop wise within 4 h to a stirred ice-cooled solution of **5** (10.0 g;

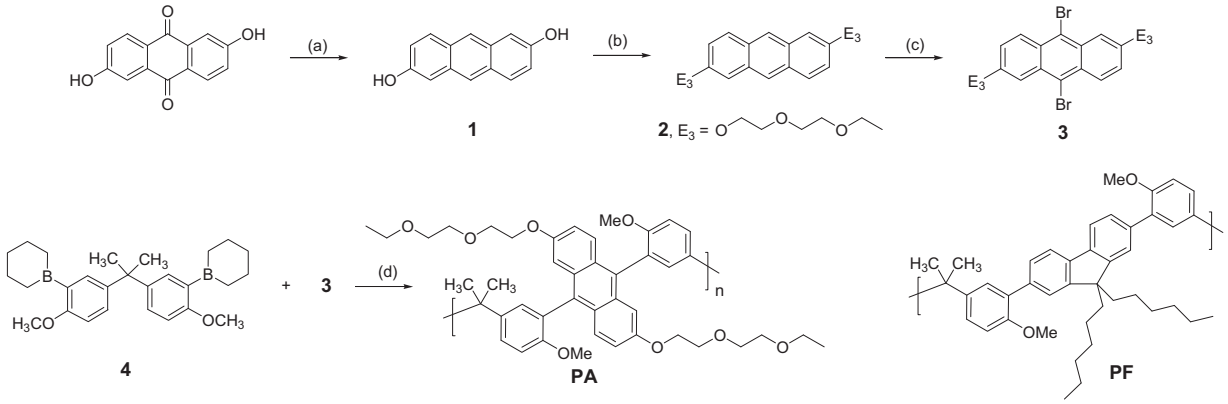

Scheme 1. Synthetic route of polymer **PA**, reagents and conditions (a) NH_3(aq.)/Al(Hg), reflux; (b) NaH/DMF, r.t. then **4**, reflux; (c) Br_2/CH_2Cl_2, 4 °C; (d) $Pd_2(dba)_3/P(o\text{-tolyl})_3/CO_3Na_2$ (aq.)/THF, 80 °C; structure of polymer **PF**.

23 mmol) in CH_2Cl_2 (380 ml). The mixture was washed with 5% $NaHCO_3$, dried and evaporated. Crystallization of the residue first from cyclohexane carbon tetrachloride mixture (5:1) and then from benzene (90 ml) afforded the monomer **3** (7.1 g, 51%). M.p. 122–123 °C. ^{1}H NMR ($CDCl_3$) *d* 8.36 (d, 1H, *J* = 9.5 Hz), 7.69 (d, 1H, *J* = 2.4 Hz), 7.28 (dd, 1H, *J* = 9.5 Hz and 2.4 Hz), 4.35 (m, 2H), 3.97 (m, 2H), 3.63 (m, 4H), 3.54 (q, 2H, *J* = 7.0 Hz), 1.21 (t, 3H, *J* = 7.0 Hz); ^{13}C NMR ($CDCl_3$) *d* 157.4, 130.7, 129.8, 127.9, 122.5, 121.3, 105.4, 71.2, 70.1, 69.8, 67.8, 66.9, 15.4; MS (70 eV), *m*/*z* (%), 602 (M^++4, 32), 600 (M^++2, 62), 598 (M^+, 32), 117 (57), 89 (18), 73 (100). Anal. Calcd. for $C_{26}H_{32}Br_2O_6$ C, 52.02; H, 5.37. Found C, 51.80; H, 5.20.

2.2.2. Polymer synthesis

The complete synthesis and characterization of polymer **PF** has been already reported [15]. The synthesis of polymer **PA** was carried out as follows A 50 ml Schlenk tube was charged with $Pd(PPh_3)_4$ (0.024 g, 0.02 mmol), **3** (1.192 g, 2.00 mmol), Na_2CO_3 (2.82 g, 26.6 mmol) and 2,2-bis[3-(1,3,2-dioxaborinan-2-yl)-4-methoxyphenyl]propane (0.824 g, 2.00 mmol) and the mixture was kept under Ar atmosphere. Dry THF (13.3 ml) and water (13.3 ml) were added via a syringe. The mixture was heated at 80 °C for 7 days. The reaction mixture was poured into methanol (30 ml). The precipitate was collected by filtration and dissolved in $CHCl_3$ (4.0 ml). The solution was filtered and poured into methanol (30.0 ml). The precipitate was collected by filtration and dried under vacuum (0.300 g, 25%). ^{1}H NMR ($CDCl_3$) *d* 7.41 (m, 2H), 7.21 (m, 1H), 7.06 (m, 1H), 6.96 (m, 1H), 6.81 (m, 1H), 4.27–3.61 (m, 6H), 1.73 (m, 1H), 1.15 (t, 3H, *J* = 6.9 Hz). ^{13}C NMR ($CDCl_3$) *d* 156.0, 155.2, 143.2, 132.1, 131.4, 128.4, 127.7, 127.3, 119.8, 113.4, 111.0, 104.0, 70.8, 69.8, 69.5, 66.9, 66.6, 55.8, 42.2, 31.9, 15.1. Anal. Calcd. For $(C_{43}H_{50}O_8)_n$ C, 74.33; H, 7.25; O, 18.42. Found C, 73.19; H, 6.91.

2.3. Molecular modeling

Molecular modeling of the dimer was carried out with the ORCA program package (3.02 ed.) [22] and using HF-3c [23]. This HF hydrid program use a small basis set MINIX, coupled with three empirical corrections, the atom-pairwise dispersion correction with the Becke–Johnson damping scheme (D3BJ) [24,25], the geometrical counterpoise correction gCP [26], and a short-ranged basis incompleteness correction, SRB. Pre- and post-processing operations were performed by using the graphical interface Gabedit 2.4.7 [27].

2.4. Fluorescence quenching studies

The films were casted onto carefully leveled quartz, glass, dodecyltrichlorosilane (DTS)-coated glass or polymeric substrates (2.4 cm × 0.8 cm) by spreading over the whole area 0.1 ml of a chloroform solution of the NAC which was first allowed to evaporate slowly in a nitrogen filled chamber and was then kept under vacuum for 12 h at room temperature. We have previously reported the preparation of (DTS)-coated glass substrates by treating the glass substrates first with piranha solution (70% H_2SO_4, 30% H_2O_2) and then with DTS in CH_2Cl_2 [28]. The thickness of cast films was measured in at least five different regions via a UV–visible interferometer (Model F20; Filmetrics, Inc.) operated in reflectance mode with a spot size of ~0.5 mm. Typical film thickness was ~0.1–0.7 μm for 0.1–0.5 wt% solutions. A typical film thickness of ~0.3 μm was used in quenching experiments. Stock solutions (10^{-3} M) of each NAC were prepared by dissolving the adequate amount of the desired NAC in 3 ml of MeOH and by completing the volume up to 10 ml with water.

Solid phase fluorescence quenching was investigated on films whose thickness was ca. 0.3 μm for the two sets of NACs at different concentrations in water. Quenching experiments were carried out by inserting diagonally the films down to two-thirds of the height of the quartz fluorescence cell to allow analyte equilibration. The 1 cm quartz cell was then filled with water (2.4 ml) and spectra were acquired by front-face (45°) detection at room temperature after the addition of microliter aliquots of the quencher solution. Each fluorescence spectrum either for **PA** (λ_{exc} = 390 nm, λ_{em} = 490 nm) or **PF** (λ_{exc} = 327 nm, λ_{em} = 390 nm) was recorded immediately after fluorescence intensity stabilization.

3. Results and discussion

3.1. Synthesis and thermal properties

The synthetic route for the anthracene-based monomer **3** and polymer **PA** as well as the structure of fluorene-based polymer **PF** are illustrated in Scheme 1. Reduction of 2,6-dihydroxyanthraquinone to the substituted anthracene **1** was accomplished in 65% yield with aluminum amalgam in a basic medium. Next, 1,4,7-trioxanonyl-*p*-toluenesulfonate was prepared and then it was used to obtain **2** under Williamson ether synthesis conditions. It is well known that the anthracene ring can be selectively dibrominated at the 9- and 10-positions, however, in the case of compound **2** the donor oligoethylenoxy groups activate toward electrophylic substitution the outer rings as well, so selective 9,10-dibromination of **2** is challenging in this case [29]. All

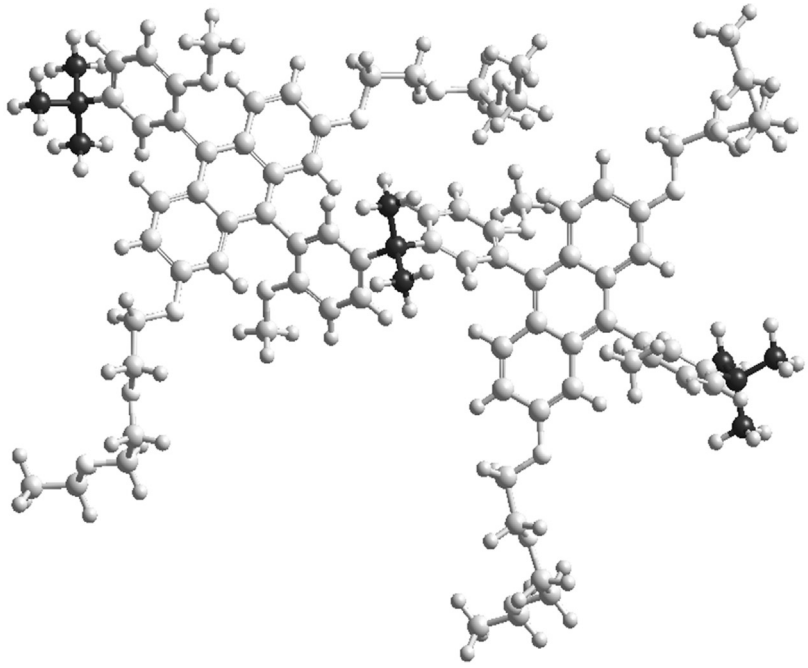

Fig. 1. HF-3c molecular model of a dimer of **PA**, the isopropylydene linking group and the two end-capping t-butyl groups are shown with black carbon atoms.

attempts done at room temperature using either higher concentrations of **2** in several organic solvents or with faster bromine addition yielded significant fractions of polybrominated products along with the desired 9,10-dibrominated derivative. Finally, selectivity was achieved by a very slow bromine addition to a cooled solution of **2** in CH_2Cl_2 which yielded **3** in acceptable yield after recrystallization (51%). The dibromide monomer **3** was then used in the preparation of polymer **PA** via palladium-catalyzed Suzuki polycondensation with comonomer **4**. Gel permeation chromatography (GPC, PS standards, THF) showed that after reprecipitation from methanol the anthrylene polymer **PA** had a monomodal distribution with a very narrow polydispersity uncommon for polycondensation reactions (M_w = 5700 Da, PDI = 1.25) albeit rather low yield (25%). Clearly, the oligooxyethylene lateral chains strongly interact with the solvent used for reprecipitation. Therefore, most polymer chains except the ones with higher mass remain in solution state. As expected, polymer **PA** was readily soluble in common organic solvents such as benzene, acetonitrile, THF and DMF, in particular this polymer is highly soluble in $CHCl_3$ (46 wt%). Its high solubility in aprotic solvents is most probably related to its non-linear structure rather than to the pending lateral chains (Fig. 1). Polymer **PA** is amorphous in nature; its DSC traces registered at a temperature range between −50 and 250 °C showed only a distinct glass transition at 82 °C and no melting transitions were found upon heating beyond the glass transition temperature. The rather low T_g temperature reflects the presence of conformationally rich oligoether side chains. Besides, no birefringence was detected for polymer **PA** by polarized optical microscopy POM observations carried out in the same temperature range. Films drop-cast on quartz plates and dried under vacuum gave smooth films suitable for optical measurements.

3.2. Photophysical and electrochemical properties

The photophysical characterization of polymer **PF** has been reported previously [15]. The absorption spectra of **PA** in dilute chloroform solution (l_{max} = 377, 396, 418 nm) and in the solid state (l_{max} = 377, 397, 419 nm) have very similar characteristics. As seen in Fig. 2, both spectra overlay and retain in fact most of the

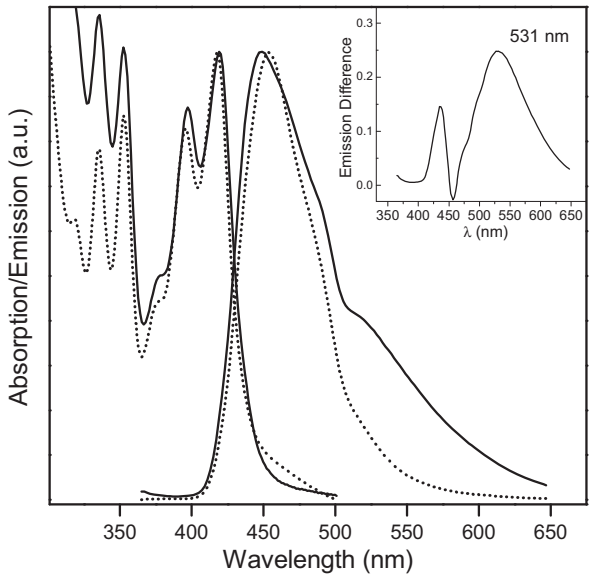

Fig. 2. (a) Normalized absorption and emission spectra (λ_{ex} = 360 nm) of $CHCl_3$ solutions (dashed curves) and films (solid curves) of **PA**. Inset: difference spectrum between the normalized emission of thin film and solution.

vibronic structure presented by the parent 2,6-diphenylanthracene chromophore indicating that the isopropylidene spacer effectively isolates the gem-chromophore units tethered into the main chain. Besides, emission spectra obtained by exciting at different energies from 420 to 450 nm on the red edge of the film absorption spectrum were similar. All these spectral features indicate that fluorescence is originated in the amorphous phase by the same species, i.e. the isolated excited chromophores, and there is minimal electronic interaction between neighboring chromophores so the presence of ground-state aggregates can be ruled out.

The fluorescence spectra of a chloroform solution (l_{max} = 453 nm, Stokes shift = 1906 cm^{-1}) and a thin film (l_{max} = 449 nm, Stokes shift = 1595 cm^{-1}) of **PA** are also shown in Fig. 1a. Despite the similarities in their fluorescence maxima, we

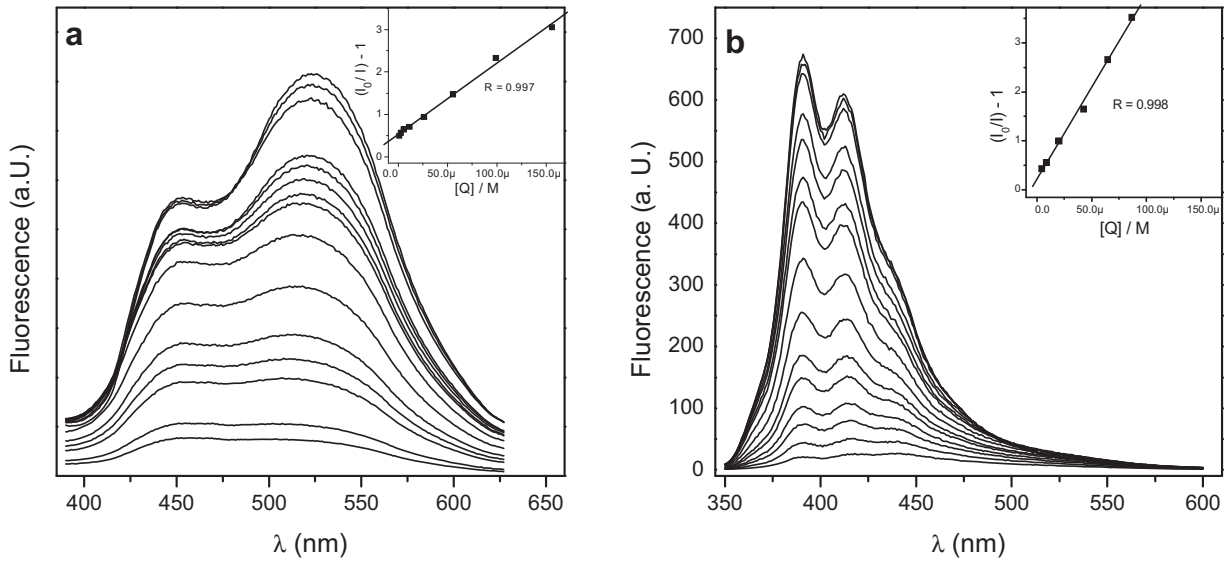

Fig. 3. (a) Fluorescence spectra change (λ_{ex} = 390 nm, λ_{em} = 450 nm) of a **PA** film as a function of added NP in water; [NP] = $1{\cdot}10^{-6}$–$1.5{\cdot}10^{-4}$ M (top to bottom). (b) Fluorescence spectra change (λ_{ex} = 327 nm, λ_{em} = 390 nm) of a **PF** film as a function of added DNP in water; [DNP] = $4{\cdot}10^{-6}$–$9{\cdot}10^{-5}$ M (top to bottom). The Stern–Volmer plots for the linear region are shown in the insets.

noticed that irradiated solutions in chloroform appear bluish green but films emit yellowish green fluorescence. Such chromatic variation seems to be originated by a new, long-wavelength emission band that appears as a shoulder in the film emission spectrum. The difference spectrum between the normalized emission of thin film and solution (Fig. 1a, inset) evidences the presence of an additional broad structureless band with an emission maximum at ca. 530 nm. The fluorescence of anthracene-based chromophores such as phenylanthracenes [30,31] and 9,9′-bianthryls [32] occasionally exhibit dual fluorescence from locally excited (LE) and charge transfer states (CT) [33–35], that is, emission emanates from either one or two equilibrated excited states of different polarities being the polar CT state favored by polar solvents. Thus, we observed that the emission in chloroform solution of polymer **PA** came exclusively from the LE state. However, the diphenylanthracene chromophores embedded into the film are surrounded by the oligooxyethylene side chains that perform as a polar covalently bound solvent which promotes formation of a small proportion of CT states causing the emission in condensed phase to become dual. Moreover, when a thin film of **PA** is submerged and soaked in water, the diffusion of water molecules into the film increases the polarity of the chromophore environment so the predominant emission comes then from the CT state (Fig. 3a). Thus, we ruled out the appearance of interchromophoric interactions such as excimers in the excited state and ascribe the differences of the emission spectra in chloroform solution and condensed state to an intrachromophoric charge transfer event.

The excited state delocalization is also relevant here because exciton migration within the film increases the frequency of interaction with quenchers thus boosting detection sensitivity. Consequently, energy migration in **PA** films was evaluated by fluorescence depolarization measurements which rendered a low residual value of the steady-state anisotropy, $\langle r \rangle = 0.074$, thus indicating good exciton mobility [10].

Cyclic voltammograms were recorded in order to obtain the oxidation potential onset of the electron-donor polymers **PA** and **PF** and then to evaluate the reducing power of their excited states by calculating their LUMO energies. The HOMO levels of the polymers were calculated from their corresponding onset oxidation potentials, E_{ox}^{onset}, and by assuming the energy level of Ag/Ag^+ to be 4.73 eV below the vacuum level [36]. The energy gap between the HOMO and LUMO levels was estimated from the edge of the UV absorption, E_g^{opt}. Then, the HOMO levels were obtained from the values of the optical band gap and the HOMO level. Measurements performed in dichloromethane solution with 0.1 M tetraethylammonium perchlorate using Ag^+/Ag as reference electrode showed that **PA** and **PF** exhibit reversible oxidations. The E_{ox}^{onset} of a **PA** film casted on a Pt electrode is 0.83 eV. For **PA** the E_g^{opt} is 2.78 eV, then HOMO = −5.56 eV and LUMO = −2.78 eV. The E_{ox}^{onset} for a film of **PF** supported on Pt was 1.36 eV. Since the E_g^{opt} of **PF** is 3.42 eV then HOMO = −6.09 and LUMO = −2.67 eV. Thus, both polymers present a very close reducing power, LUMO ∼−2.7 eV, despite the structural differences of their chromophores.

3.3. Photoluminescence quenching

The steady-state quenching experiments were done using films of polymer **PA** and **PF**. The films of **PF** were prepared onto untreated glass or quartz plates by drop-casting from chloroform solutions followed by vacuum drying while the films of polymer **PA** were casted onto dodecyltrichlorosilane (DTS)-coated glass substrates. We observed that layers of **PA** deposited onto polymeric substrates such as polyvinylacetate or PMMA, quartz and untreated glass degraded and peeled off when they were immersed in water. However, the introduction of a monolayer of nonpolar aliphatic chains that reduced in large extent the water affinity of the glass surface rendered mechanically stable films. Thus, fluorescence control experiments showed that using the pre-treated glass substrates for polymer **PA** there was no polymer leakage from the film toward the aqueous media even after 24 h and similar results were obtained for films of **PF** deposited on quartz or untreated glass substrates. We also observe that in both cases the wetting process decreased ∼20–25% the fluorescence intensity of the neat film. The pristine films were first immersed in water and allowed to hydrate, and then their steady-state fluorescence response to increasing concentrations of various analytes was observed for aqueous solutions of 4-nitrophenol (NP), 2,4-dinitrophenol (DNP), 2,4,6-trinitrophenol (TNP), 4-nitrotoluene (NT) 2,4-dinitrotoluene (DNT) and 2,4,6-trinitrotoluene (TNT). Fig. 2 displays the quenching of the luminescence spectrum of **PA** and **PF** upon addition of microliter aliquots of NACs. The plots of the Stern–Volmer (S–V)

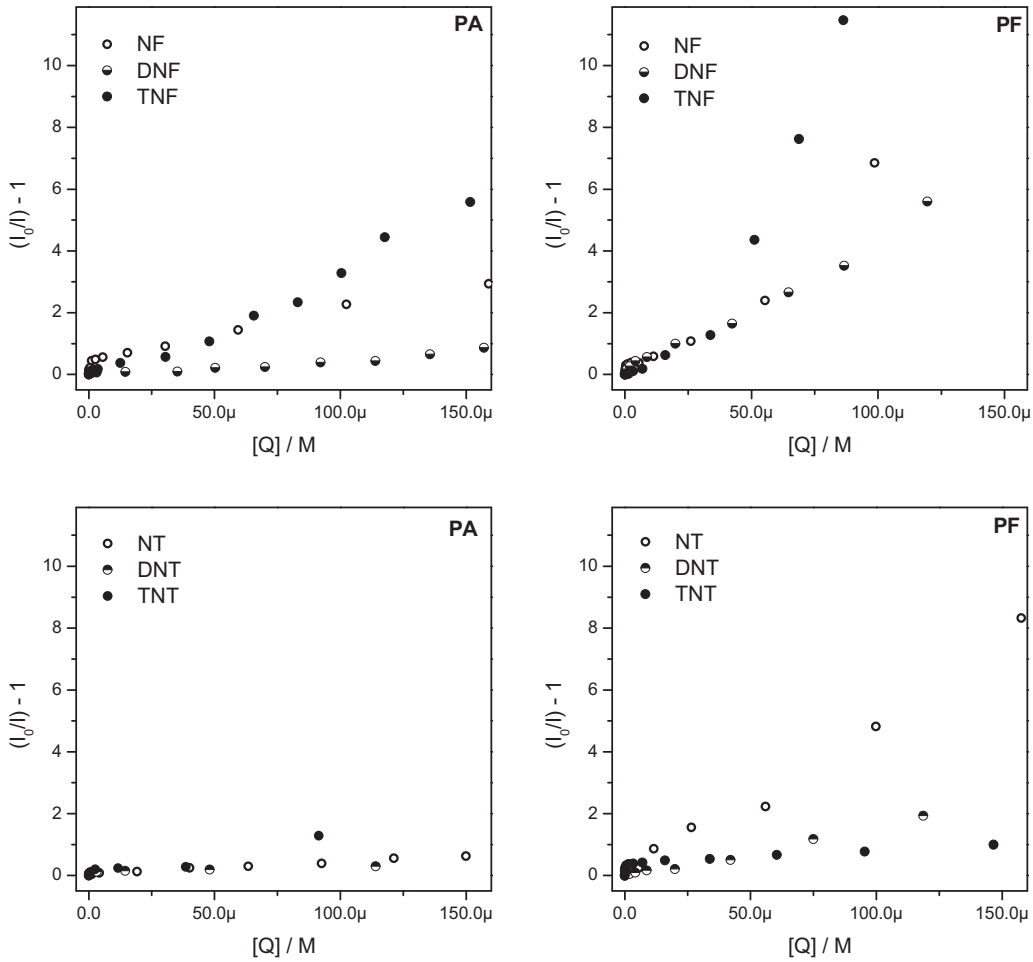

Fig. 4. Stern–Volmer plots of **PA** and **PF** in response to NP, DNP, TNP, NT, DNT and TNT.

equation, $(I_o/I) - 1 = K_{SV}[Q]$, for fluorescence quenching are shown in Fig. 3a (inset) and Fig. 3b (inset). Linear relationships with excellent correlation coefficients above 0.99 were observed for all the NACs tested albeit only in the range ~20 to ~70% of fluorescence quenching. As shown in Fig. 3, at the higher end of quencher concentrations a non-linear S–V relationship with upward curvature occurred. Comparable upward deviations from linearity have been previously determined in solid/solution sensing configurations by us [15,16] and other research groups [37,38] as well as in nanoaggregated polymers [39] and polyelectrolytes [6]. For traditional electron transfer fluorescence quenching between small molecules in solution it is customary to analyze the non-linear behavior in term of concomitant static and dynamic quenching processes [40]. However, nonlinear results observed for polyelectrolyte solutions in low good solvent/poor solvent ratios or with added cations have been frequently interpreted in terms of macromolecular aggregation that enhances quenching due to interchain exciton migrations [6,7]. In solid/solution sensing configurations, the molecular or macromolecular fluorophores are aggregated by definition, therefore they likely present quenching phenomena similar to that of aggregated macromolecules in solution. Moreover, in our previous work we found that the same upward curvature in quenching experiments was displayed by 9 nm and 35 nm thin films as well as by thicker films, thereby indicating that analyte diffusion into the polymer layer does not bear upon the non-linear quenching response. Hence the upwards curvatures shown in Fig. 4 are most probably due to increasingly efficient quenching of migrants excitons as the analyte concentration augments.

The S–V constant (K_{SV}) and the values of half of the maximum quench, $Q_{50\%}$, that is, the quencher concentration needed to reach $(I_o/I) - 1 = 1$ as well as the values for almost complete quenching, $Q_{90\%}$, are summarized in Table 1 and Fig. 4. These data show several general features worthy of discussion. First, hydrated films of the two electrodonor polymers exhibit remarkable sensing abilities for all electrodeficient nitrophenols and nitrotoluenes in aqueous media, showing $Q_{50\%}$ in the micromolar range and almost complete quenching, $Q_{90\%}$, at the milimolar range, thus showing facile analyte diffusion into the polymers, a clear indication that the hydrated films of the two polymers have porosity at the molecular level. Secondly, the fluorene-based **PF** had higher overall quenching responses to NACs than anthryl-based **PA** with the exception of TNT, that is, **PA** was nearly three times more sensitive toward TNT than **PF**. In third place, nitrophenols were more effective than nitrotoluenes in quenching the fluorescence of both **PA** and **PF**.

The fluorescence quenching of a CPs in solution depends initially on the thermodynamic driving force for the photoinduced electron transfer which is generally discussed for a given polymer in terms of the reduction potential of NACs but exceptions exist to this simple correlation because steric effects could hinder the close approach of the analyte or the polymer hydrodynamic volumes can be influenced by the quencher or the solvent [17,41]. On the other hand, solid state quenching efficiency of NACs vapors usually follows the vapor pressure values of NACs but is also affected by the molecular volume of the analyte, polymer–analyte electrostatic interactions and polymer morphology that affect the diffusion rates of analytes within the film [2,7]. Our sensing configuration

Table 1
Data analysis of Stern–Volmer plots and quenching efficiencies.

Quencher (Q)	**PA**			**PF**		
	K_{SV}, M^{-1}	$Q_{50\%}$, μM[a]	$Q_{90\%}$, μM[b]	K_{SV}, M^{-1}	$Q_{50\%}$, μM[a]	$Q_{90\%}$, μM[b]
NP	16,700	34	377	40,500	23	115
DNP	8530	170	478	43,100	20	170
TNP	17,700	47	180	39,000	27	80
NT	4740	200	1100	45,100	16	180
DNT	1510	450	1400	16,700	62	490
TNT	12,350	70	260	4530	150	1200

[a] [Q] for $(I_o/I) - 1 = 1$.
[b] [Q] for $(I_o/I) - 1 = 9$.

Table 2
Solubility parameters, HSP, and solubility parameter distances, *Ra*, for NACs and polymers **PA** and **PF**.

	HSP			**PA** vs NAC				**PF** vs NAC			
	δ_d	δ_p	δ_{hb}	$\Delta\delta_d$	$\Delta\delta_p$	$\Delta\delta_{hb}$	Ra[a]	$\Delta\delta_d$	$\Delta\delta_p$	$\Delta\delta_{hb}$	Ra[a]
NP	19.6	10.8	12.5	5.5	−2.8	−11.4	16.1	4.9	−5.0	−11.1	15.7
DNP	20.2	15.9	12.1	4.8	−2.2	−11.1	14.8	4.3	−10.1	−10.7	17.0
TNP	21.7	20.9	11.8	3.4	−7.3	−10.7	14.6	2.8	−15.1	−10.3	19.2
NT	19.2	9.1	4.4	5.8	4.5	−3.3	12.9	5.1	−3.4	−3.0	11.5
DNT	20.5	14.2	4.0	4.5	−0.6	−2.9	9.5	4.0	−8.4	−2.6	11.9
TNT	21.5	19.2	3.7	3.5	−5.6	−2.6	9.3	3.0	−13.4	−2.2	14.9

[a] Calculated using the following HSP for **PA** (δ_d = 25.0, δ_p = 13.6, δ_{hb} = 1.1) and **PF** (δ_d = 24.5, δ_p = 5.8, δ_{hb} = 1.5).

consists of a hydrated polymer film in contact with the quencher solution so correlations with the reduction potential of NACs and factors controlling the diffusion of NACs into the film could be expected. But, keeping in mind that reduction potential decreases and the volume increases with the number of nitro groups, we conclude that K_{SV} constants did not follow clear trends in terms of quencher electronic or steric characteristics either for **PA** or **PF**, i.e., K_{SV} of **PA** for nitrophenols follows the order of NP ∼ TNP > DNP and TNT > NT > DNT while **PF** showed a high sensibility toward nitrophenols but no selectivity, that is, the quenching efficiency order was NP ∼ DNP ∼ NP. On the other hand, the quenching constant of nitrotoluenes diminishes in the order of NT, DNT and TNT. Therefore, being both polymers amorphous with close glass transition temperatures ($T_{g\mathbf{PA}}$ = 82 °C and $T_{g\mathbf{PF}}$ = 95 °C), having reductive excited states of similar energy (LUMO ∼ 2.7 eV) and presenting alike relevant optical response, i.e., the low residual steady-state anisotropies values in solid phase showed good exciton mobility by homo resonance energy transfer, $\langle r \rangle_{\mathbf{PA}} = 0.074$) and $\langle r \rangle_{\mathbf{PF}} = 0.046$ [15], we focus on the binding strength between analyte and sensing material, i.e., the compatibility between polymer **PA** with polar side chains and polymer **PF** with the two sets of NACs.

An established method to assess molecular interactions is the comparison of their Hansen solubility parameters (HSPs) [42–45]. Hansen's method [46] rests upon the concept that the cohesive energy density (or the square of the total solubility parameter, ced = δ_t^2) of a neat compound is the sum of squares of the partial solubility parameters for the atomic dispersive interactions, permanent dipole molecular interactions, and hydrogen-bonding interactions.

$$\text{ced} = \delta_t^2 = \delta_d^2 + \delta_p^2 + \delta_{hb}^2$$

where δ_d, δ_p and δ_{hb} are the dispersion HSP, polar HSP and hydrogen-bonding HSP.

According to this approach, the closer the parameters of two interacting species are in the three-dimensional Hansen solubility scale, the higher the solubility is. Thus, the solubility parameter distance, R_a, quantifies the similarity in cohesive energy between a polymer and a analyte. In the present case, the solubility difference between the polymers and NACs will be expressed by the following equation

$$R_a = [4(\delta_{d,polym} - \delta_{d,NAC})^2 + (\delta_{p,polym} - \delta_{p,NAC})^2 + (\delta_{hb,polym} - \delta_{hb,NAC})^2]^{1/2}$$

Therefore, the Hansen solubility parameters, HSPs, of the nitroaromatic analytes were calculated using an updated version [47] of the Stefanis–Panayiotou group-contribution method [48] which is based on a statistical thermodynamic approach [49]. Similarly, calculations of the components of the solubility parameters of polymers **PA** and **PF** were performed and their solubility differences R_a with the NACs were then evaluated. This data is shown in Table 2. Taking into consideration that the smaller the R_a, the better the binding strength for a given polymer–analyte combination, then the R_a values indicate that as a general trend both the nitrophenols and nitrotoluenes tested here are more soluble in polymer **A** than in **F** while the relative compatibilities of nitrophenols with both polymers **A** and **F** are lower than those of the nitrotoluenes. In fact, nitrotoluenes and nitrophenols showed higher quenching sensitivities for the less compatible polymer **F** with alkyl chains, while the less compatible nitrophenol set was more effective in quenching both **PA** and **PF** than the nitrotoluene set. Apparently, analyte cohesive interactions with the polymers could drag analyte diffusion and harm the polymer sensing ability.

3.4. Conclusions

A new regularly segmented conjugated polymer with diphenylanthryl chromophores bearing oxyethylene side chains was synthesized by Suzuki cross-coupling. The polymer was solution-processable, presented amorphous morphology and formed homogeneous transparent films with stable optical properties. The formation of aggregated species in solid phase was hindered by the bent microstructure. Fluorescence depolarization measurements in condensed phase showed high exciton mobilities among the short chromophores. The fluorescence quenching response of films of **PA** to nitrophenols and nitrotoluenes in aqueous solution was evaluated and compared with the response obtained for **PF**; a diphenylfluorenylene-based segmented CP bearing non-polar aliphatic side chain. Films of the two electrodonor polymers

exhibit remarkable sensing abilities in the micromolar range for all NACs in aqueous media. Total quenching showed that hydrated films of the two polymers have porosity at the molecular level. The fluorene-based **PF** had higher overall quenching responses to NACs than anthryl-based **PA** while nitrophenols were more effective than nitrotoluenes in quenching the fluorescence of both **PA** and **PF**. Such differences are rationalized in terms of polymer–analyte interactions. Thus, the binding strengths between sensing materials and analytes were evaluated by comparison of their Hansen solubility parameters. We concluded that analyte cohesive interactions with the polymer could drag analyte diffusion and impair polymer sensing ability. Therefore the existence of strong specific or non-specific electrostatic interactions should be avoided in the design of responsive polymers to be used in the present sensing configuration.

Acknowledgments

Financial support from SGCyT-UNS, CIC-PBA and CONICET is acknowledged. MJR thanks CONICET for a fellowship. MFA is member of the research staff of CIC-PBA. PGDR, CB and ROG are members of the research staff of CONICET.

References

[1] J.S. Caygill, F. Davis, S.P.J. Higson, Current trends in explosive detection techniques, Talanta 88 (2012) 14–29.
[2] A.I. Costa, H.D. Pinto, L.F.V. Ferreira, J.V. Prata, Solid-state sensory properties of CALIX-poly(phenylene ethynylene)s toward nitroaromatic explosives, Sens. Actuators B: Chem. 161 (2012) 702–713.
[3] R. Mantha, K.E. Taylor, N. Biswas, J.K. Bewtra, A continuous system for Fe^0 reduction of nitrobenzene in synthetic wastewater, Environ. Sci. Technol. 35 (2001) 3231–3236.
[4] M.A. Rubio, E. Lissi, N. Herrera, V. Pérez, N. Fuentes, Phenol and nitrophenols in the air and dew waters of Santiago de Chile, Chemosphere 86 (2012) 1035–1039.
[5] M.R. Islam, Z. Lu, X. Li, A.K. Sarker, L. Hu, P. Choi, X. Li, N. Hakobyan, M.J. Serpe, Responsive polymers for analytical applications: a review, Anal. Chim. Acta 789 (2013) 17–32.
[6] Y. Liu, K. Ogawa, K.S. Schanze, Conjugated polyelectrolytes as fluorescent sensors, J. Photochem. Photobiol. C: Photochem. Rev. 10 (2009) 173–190.
[7] S.W. Thomas, G.D. Joly, T.M. Swager, Chemical sensors based on amplifying fluorescent conjugated polymers, Chem. Rev. 107 (2007) 1339–1386.
[8] S. Rochat, T.M. Swager, Conjugated amplifying polymers for optical sensing applications, ACS Appl. Mater. Interfaces 5 (2013) 4488–4502.
[9] G. Tang, S.S.Y. Chen, P.E. Shaw, K. Hegedus, X. Wang, P.L. Burn, P. Meredith, Fluorescent carbazole dendrimers for the detection of explosives, Polym. Chem. 2 (2011) 2360–2368.
[10] M. Guo, O. Varnavski, A. Narayanan, O. Mongin, J.-P. Majoral, M. Blanchard-Desce, T. Goodson III, Investigations of energy migration in an organic dendrimer macromolecule for sensory signal amplification, J. Phys. Chem. A 113 (2009) 4763–4771.
[11] J. Liu, Y. Zhong, P. Lu, Y. Hong, J.W.Y. Lam, M. Faisal, Y. Yu, K.S. Wong, B.Z. Tang, A superamplification effect in the detection of explosives by a fluorescent hyperbranched poly(silylenephenylene) with aggregation-enhanced emission characteristics, Polym. Chem. 1 (2010) 426–429.
[12] S. Zhang, F. Lu, L. Gao, L. Ding, Y. Fang, Fluorescent sensors for nitroaromatic compounds based on monolayer assembly of polycyclic aromatics, Langmuir 23 (2007) 1584–1590.
[13] G. He, G. Zhang, F. Lu, Y. Fang, Fluorescent film sensor for vapor-phase nitroaromatic explosives via monolayer assembly of oligo(diphenylsilane) on glass plate surfaces, Chem. Mater. 21 (2009) 1494–1499.
[14] P.G. Del Rosso, M.F. Almassio, P. Aramendia, S.S. Antollini, R.O. Garay, Poly[(2,2,5,2-tetramethoxy-p-terphenyl-5,5-ylene)propylene]: synthesis and physical properties of a novel amorphous regularly segmented conjugated polymer, Eur. Polym. J. 43 (2007) 2584–2593.
[15] P.G. Del Rosso, M.F. Almassio, G.R. Palomar, R.O. Garay, Nitroaromatic compounds sensing. Synthesis, photophysical characterization and fluorescence quenching of a new amorphous segmented conjugated polymer with diphenylfluorene chromofores, Sens. Actuators B: Chem. 160 (2011) 524–532.
[16] P.G. Del Rosso, M.F. Almassio, R.O. Garay, Chemosensing of nitroaromatics with a new segmented conjugated quaterphenylene polymer, Tetrahedron Lett. 52 (2011) 4911–4915.
[17] D. Zhao, T.M. Swager, Sensory responses in solution vs solid state a fluorescence quenching study of poly(iptycenebutadiynylene)s, Macromolecules 38 (2005) 9377–9384.
[18] M. Ranger, D. Rondeau, M. Leclerc, New well-defined poly(2,7-fluorene) derivatives: photoluminescence and base doping, Macromolecules 30 (1997) 7686–7691.
[19] M. Sunagawa, H. Matsumara, Y. Kitamara, Crystalline palladium tetrakis(triphenyl-phosphine) and process for preparing the same, European Patent 0493032A2, Sumimoto Pharmaceuticals Company (1991).
[20] W.H. Dennis Jr., D.H. Rosenblatt, W.G. Blucher, C.L. Coon, Improved synthesis of TNT isomers, J. Chem. Eng. Data 20 (1975) 202–203.
[21] R.W. Lenz, A. Furukawa, P.K. Bhowmik, R.O. Garay, J. Majnusz, Synthesis and characterization of extended-rod thermotropic polyesters with polyoxyethylene pendant substituents, Polymer 32 (1991) 1703–1712.
[22] F. Neese, The ORCA program system, Wiley Interdiscip. Rev. Comput. Mol. Sci. 2 (2012) 73–78.
[23] R. Sure, S. Grimme, Corrected small basis set Hartree–Fock method for large systems, J. Comput. Chem. 34 (2013) 1672–1685.
[24] S. Grimme, S. Ehrlich, L. Goerigk, Effect of the damping function in dispersion corrected density functional theory, J. Comput. Chem. 32 (2011) 1456–1465.
[25] S. Grimme, J. Antony, S. Ehrlich, H. Krieg, A consistent and accurate *ab initio* parametrization of density functional dispersion correction (DFT-D) for the 94 elements H–Pu, J. Chem. Phys. 132 (2010) 154104.
[26] H. Kruse, S. Grimme, A geometrical correction for the inter- and intra-molecular basis set superposition error in Hartree–Fock and density functional theory calculations for large systems, J. Chem. Phys. 136 (2012) 154101.
[27] A.R. Allouche, Gabedit – a graphical user interface for computational chemistry softwares, J. Comp. Chem. 32 (2011) 174–182.
[28] C.M. Hegguilustoy, R.S. Montani, M.B. Darda, P.G. Del Rosso, R.O. Garay, Bent-shaped liquid crystal dimers. Influence of the direction of the oxybiphenylenecarboxyl groups on their mesomorphic behavior, ARKIVOC vii (2011) 283–296.
[29] D.W. Cameron, P.E. Schütz, Some halogenated derivatives of 2,6-dihydroxyanthracene, J. Chem. Soc. C (1967) 2118–2120.
[30] Z.R. Grabowski, K. Rotkiewicz, Structural changes accompanying intramolecular electron transfer focus on twisted intramolecular charge-transfer states and structures, Chem. Rev. 103 (2003) 3899–4031.
[31] J.V. Lockard, A. Butler Ricks, D.T. Co, M.R. Wasielewski, Interrogating the intramolecular charge-transfer state of a julolidin–anthracene donor–acceptor molecule with femtosecond stimulated Raman spectroscopy, J. Phys. Chem. Lett. 1 (2010) 215–218.
[32] R. Yamakado, S.-I. Matsuoka, M. Suzuki, D. Takeuchi, H. Masu, I. Azumaya, K. Takagi, Synthesis, reaction, and optical properties of cyclic oligomers bearing 9,10-diphenylanthracene based on an aromatic tertiary amide unit, RSC Adv. 4 (2014) 6752–6760.
[33] R. Fritz, W. Rettig, K. Nishiyama, T. Okada, U. Müller, Klaus Müllen, Excitonic and charge transfer states in oligomeric 9,10-anthrylene chains, J. Phys. Chem. A 101 (1997) 2796–2802.
[34] F.C. Grozema, M. Swart, R.W.J. Zijlstra, J.J. Piet, L.D.A. Siebbeles, P. Th van Duijnen, QM/MM study of the role of the solvent in the formation of the charge separated excited state in 9,9′-bianthryl, J. Am. Chem. Soc. 127 (2005) 11019–11028.
[35] P. Natarajan, M. Schmittel, Photoluminescence, Redox properties, and electrogenerated chemiluminescence of twisted 9,9′-bianthryls, J. Org. Chem. 78 (2013) 10383–10394.
[36] M. Thelakkat, H.-W. Schmidt, Synthesis, Properties of novel derivatives of 1,3,5-tris(diarylamino)benzenes for electroluminescent devices, Adv. Mater. 10 (10) (1998) 219–223.
[37] D. Patra, A.K. Mishra, Fluorescence quenching of benzo[k]fluoranthene in poly(vinyl alcohol) film a possible optical sensor for nitro aromatic compounds, Sens. Actuators B: Chem. 80 (2001) 278–282.
[38] J. Feng, Y. Li, M. Yang, Conjugated polymer-grafted silica nanoparticles for the sensitive detection of TNT, Sens. Actuators B: Chem. 145 (2010) 438–443.
[39] A. Qin, J.W.Y. Lam, L. Tang, C.K.W. Jim, H. Zhao, J. Sun, B.Z. Tang, Polytriazoles with aggregation-induced emission characteristics synthesis by click polymerization and application as explosive chemosensors, Macromolecules 42 (2009) 1421–1424.
[40] B. Valeur, Molecular Fluorescence, Wiley-VCH, Weinheim, Germany, 2001.
[41] H. Sohn, M.J. Sailor, D. Magde, W.C. Trogler, Detection of nitroaromatic explosives based on photoluminescent polymers containing metalloles, J. Am. Chem. Soc. 125 (2003) 3821–3830.
[42] F. Machui, S. Langner, X. Zhu, S. Abbott, C.J. Brabec, Determination of the P3HT PCBM solubility parameters via a binary solvent gradient method: impact of solubility on the photovoltaic performance, Sol. Energy Mater. Sol. Cells 100 (2012) 138–146.
[43] B. Walker, A. Tamayo, D.T. Duong, X.-D. Dang, C. Kim, J. Granstrom, T.-Q. Nguyen, A systematic approach to solvent selection based on cohesive energy densities in a molecular bulk heterojunction system, Adv. Energy Mater. 1 (2011) 221–229.
[44] Y. Hernandez, M. Lotya, D. Rickard, S.D. Bergin, J.N. Coleman, Measurement of multicomponent solubility parameters for graphene facilitates solvent discovery, Langmuir 26 (2010) 3208–3213.
[45] D.L. Olynick, P.D. Ashby, M.D. Lewis, T. Jen, H. Lu, J.A. Liddle, W. Chao, The link between nanoscale feature development in a negative resist and the Hansen solubility sphere, J. Polym. Sci. B: Polym. Phys. 47 (2009) 2091–2105.
[46] C.M. Hansen, Hansen Solubility Parameters: A Users Handbook, 2nd ed., CRC Press LLC, Boca Raton, FL, 2007.
[47] E. Stefanis, C. Panayiotou, A new expanded solubility parameter approach, Int. J. Pharm. 426 (2012) 29–43.

[48] E. Stefanis, C. Panayiotou, Prediction of Hansen solubility parameters with a new group-contribution method, Int. J. Thermophys. 29 (2008) 568–585.
[49] C. Panayiotou, Statistical thermodynamic calculations of the hydrogen bonding, dipolar, and dispersion solubility parameters, in: C.M. Hansen (Ed.), Hansen Solubility Parameters: A Users Handbook, 2nd ed., CRC Press LLC, Boca Raton, FL, 2007.

Biographies

Pablo G. Del Rosso received his Ph.D. in chemistry from the Universidad Nacional del Sur (UNS) in 2006. He did postdoctoral work at the Max-Planck Institut für Polymerforschung with Prof. K. Müllen from 2007 to 2008. He holds a permanent position as Assistant Professor in the Departamento de Química at UNS since 2011. His research interests are mainly focused in the synthesis and applications of organic conjugated materials.

María J. Romagnoli received his B.Sc. from Universidad Nacional de La Plata in 2012. In the same year she joined Prof. Raul O. Garay's group as a Ph.D. student at the Universidad Nacional del Sur where she is doing studies in responsive polymer-based materials for sensing applications.

Marcela F. Almassio received his Ph.D. in chemistry from the Universidad Nacional del Sur (UNS) in 2007. He did postdoctoral work at the University of Coimbra with Prof. S. Seixas de Melo from 2010 to 2011. He holds a permanent position as Instructor in the Departamento de Química at UNS since 2006. Her research interests are mainly focused in the synthesis and electrooptical characterizations of organic and bioorganic materials.

Cesar Barbero received his PhD in chemistry from the Universidad Nacional de Rio Cuarto (UNRC) in 1988. He did postdoctoral work at the Paul Scherrer Institut with Prof O. Haas from 1988 to 1994. He is Full Professor at the Departamento de Química at UNRC since 2005. His group's research program is focused on developing probe beam deflection techniques, porous carbon materials and hierarchical systems as well as nanocomposites made of conducting nanoparticles and smart hydrogels.

Raúl O. Garay received his Ph.D. in chemistry from the Universidad Nacional del Sur (UNS) in 1985. After postdoctoral work in the Department of Polymer Science & Eng. at UMASS with Prof. R.W. Lenz, at the Max-Planck Institut für Polymerforschung and BASF with Prof. K. Müllen from 1988 to 1993, he was a Lecturer A at UMASS from 1993 to 1994. He is Full Professor at the Departamento de Química at UNS since 1995. His research interests are in the areas of luminescent conjugated polymers and thermotropic liquid crystals.